Talanta 84 (2011) 673–678

Contents lists available at ScienceDirect

Talanta

journal homepage: www.elsevier.com/locate/talanta

Synthesis of silver nanowires and their applications in the electrochemical detection of halide

Xia Qin[a,c], Huicai Wang[b,**], Zhiying Miao[a], Xinsheng Wang[a], Yuxin Fang[a], Qiang Chen[a,*], Xueguang Shao[c]

[a] *The Key Laboratory of Bioactive Materials, Ministry of Education, College of Life Science, Nankai University, Tianjin 300071, China*
[b] *State Key Laboratory of Hollow Fiber Membrane Materials and Process, Tianjin Polytechnic University, Tianjin 300160, China*
[c] *College of Chemistry, Nankai University, Tianjin 300071, China*

ARTICLE INFO

Article history:
Received 13 October 2010
Received in revised form 23 January 2011
Accepted 27 January 2011
Available online 2 February 2011

Keywords:
Silver nanowires
Halide ions
Simultaneous detection
Cyclic voltammetry

ABSTRACT

A silver nanowires modified platinum (Ag NWs/Pt) electrode was developed for simultaneous and selective determination of chloride, bromide and iodide ions by cyclic voltammetry in aqueous solutions. Silver nanowires were synthesized by an L-cysteine-assisted poly (vinyl pyrrolidone) (PVP)-mediated polyol route. X-ray diffraction (XRD) and scanning electron microscopy (SEM), transmission electron microscopy (TEM) and energy dispersive X-ray spectroscopy (EDS) were employed to investigate the prepared nanowires. The intrinsic high surface area and the fast electron transfer rate ascribed from the nanowire structure could further improve halide detection performance. The determination was based on measurement of the well-separated oxidation peak currents of respective silver halides formed on the surface of silver during an anodic potential sweep. The concentration range was linear from 50 μM to 20.2 mM for bromide and iodide and 200 μM to 20.2 mM for chloride, and the sensitivity was 0.059 μA/mM, 0.042 μA/mM and 0.032 μA/mM for chloride, bromide and iodide, respectively. The correlation coefficient was 0.999 in each case. The Ag NWs/Pt electrode offered a useful platform for the development of a highly sensitive halide sensor.

1. Introduction

Due to their unique and interesting properties that are not seen in bulk or three-dimensional (3-D) materials, 1-D nanomaterials (wires, rods, tubes and dendrites) have been extensively explored [1–4]. Above all, considerable attention has been paid to nanowires, which are considered as building blocks for the next generation of electronics, photonics, sensors and energy applications [5,6]. Nanowires based biosensors exhibited improved signal-to-noise ratio, high faradaic current density, fast electron transfer rate, enhanced sensitivity, and low detection limit [7–9]. The excellent properties of nanowires are due to several beneficial features in the electrochemical reaction on electrodes [10,11]: (i) facile pathways for the electron transfer and (ii) effective surface exposure in the electrode–electrolyte interface, both of which are particularly important in electrochemical sensors.

Many methods have been developed to synthesize silver nanowires in hard templates [12,13] and soft templates [14,15]. Herein, we reported a method to prepare silver nanowires with an average diameter of about 300 nm by an L-cysteine-assisted poly (vinyl pyrrolidone) (PVP)-mediated polyol process. And we moved on to explore the potential applications of the silver nanowires in electroanalysis of halide ions.

Determination of halide ions is an important need in clinical diagnosis, environmental monitoring, and industrial applications [16–18]. The coulometric titration method [19], Shales and Shales method [20], and the ion-selective electrode (ISE) method [21,22] have long been used for halide sensing. Although the performances of these methods are notable, their selectivity and sensitivity remain as drawbacks [23,24]. Therefore, selective and sensitive detection of halide was highly desired. In recent years, underpotentially deposited (UPD) Ag adlayers on Au(III) surfaces with an effected electrochemical change by halide adsorption was reported to determine halide ions [24–27]. Yet, this method is time-consuming in some extent since a contact time for adsorptive accumulation of halide ions was required. Voltammetric determination method with well-separated redox peaks of different silver halides was also reported as a sensitive and selective way to detect halide ions, using silver substrate as the sensing agent [28,29]. It is proposed that, as a halide ion reacts with Ag, a silver halide precipitate is formed on the surface. The reversible potentials caused from the oxidation and reduction of the silver halides

---

* Corresponding author. Tel.: +86 22 23507273; fax: +86 22 23506122.
** Corresponding author. Tel.: +86 22 24528172; fax: +86 22 23506122.
E-mail addresses: wanghc@nankai.edu.cn (H. Wang), qiangchen@nankai.edu.cn (Q. Chen).

0039-9140/$ – see front matter © 2011 Elsevier B.V. All rights reserved.
doi:10.1016/j.talanta.2011.01.064

on the electrode surface provide a possibility for halide sensing, and the current–potential relationship could be used to identify the type of halide and its concentration. Such an approach provides several advantages over conventional ISE-based sensors for halide detection in which membranes are used for their selectivity. These benefits include direct contact between the solution and the electrode surface (i.e., no diffusional barrier), a high electrode affinity for halide ions, time saving and an approach that affords straightforward microsensor fabrication. However, to the best of our knowledge, only bulk Ag was used in the voltammetric method, for instance, Arai et al. [28] used a one-body type silver electrode and Chiu et al. [29] developed a screen-printed silver electrode to analyze halides, while a report based on nanostructured silver has not been seen.

In this study, attention was directed to the separation and detection of halide ions by voltammetry using the silver nanowires modified Pt (Ag NWs/Pt) electrode. The electrode might be gifted with critical features of high surface area and fast electron transfer rate from the nanowire structure, which could further improve halide detection performance. The method was shown to be applicable to the separate determination of chloride, bromide and iodide ions with good sensitivity and selectivity.

2. Experimental methods

2.1. Reagents and materials

Sliver nitrate ($AgNO_3$) was purchased from Tianjin Yingda Rare Chemical Reagent Company. Poly (vinyl pyrrolidone) (PVP, *K* value: 29–32) was obtained from Sigma–Aldrich Co., L-cysteine was purchased from Fluka Co. KBr and KCl were obtained from Tianjin Damao Chemical Reagent Company. KI was obtained from Tianjin Yingda Rare Chemical Reagent Company. A 0.1 M stock solution of Cl^-, Br^- and I^- were prepared with 0.1 M phosphate buffer solution (PBS) (pH 7.0) and stored under refrigeration. All other reagents were of analytical grade and used without further purification. All aqueous solutions were prepared with doubly distilled water. All experiments were performed at room temperature, approximately 25 °C.

2.2. Synthesis of silver nanowires

Silver nanowires were prepared by an L-cysteine assisted PVP-mediated polyol process. In a typical synthesis procedure, 5 mL ethylene glycol (EG) was first injected into a 50 mL three-necked flask and preheated for 10 min at 160 °C. Then 5 mL EG solution of $AgNO_3$ (1 M) was injected within 10 s while 5 mL EG solution of poly (vinyl pyrrolidone) (PVP) (3 M) containing 1 mM of L-cysteine was injected dropwise within 10 min. The reaction was kept for another 20 min. The final product was washed with acetone, ethanol and water by centrifugation at 3000 rpm for 5 min to remove the possible contamination. Considering that the silver nanowires would not be dispersed well when it is more concentrated, the purified silver nanowires were suspended in water with concentration of 10 mg/mL for characterization.

2.3. Fabrication of the halide sensor

Pt electrode (3 mm diameter) was polished with aluminum oxide nanopowder, washed ultrasonically in ethanol and doubly distilled water, and then the Pt electrode was electrochemically pretreated using potential cycling between −600 and +1000 mV vs. Ag/AgCl in 0.5 M H_2SO_4, until a steady state was reached. A certain amount of silver nanowires suspension was dropped onto the surface of the prepared Pt electrode, after drying the Ag NWs/Pt electrode was obtained.

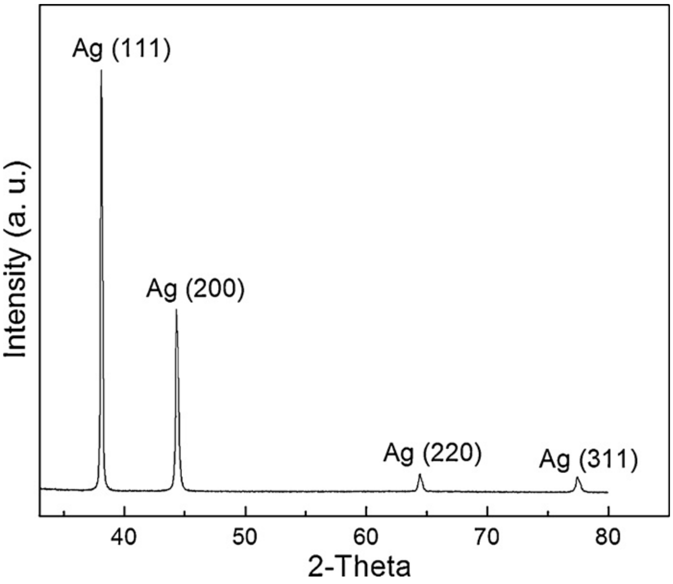

Fig. 1. XRD pattern of the as prepared silver nanowires.

2.4. Instrumentation and characterization

The electrochemical measurements were performed at room temperature in a conventional one compartment cell using a 283 Potentiostat–Galvanostat electrochemical workstation (EG&G PARC with a software M270) linked to a personal computer for data acquisition and potential control. A conventional three-electrode system comprising the Ag NWs modified Pt electrode (3 mm diameter) as a working electrode, a Pt wire (1 mm diameter) as an auxiliary electrode and an Ag/AgCl (saturated with KCl) as a reference electrode was employed for all electrochemical experiments.

The X-ray diffraction (XRD) patterns were recorded using a Rigaku D/max-rA with Cu Kα radiation ($\lambda = 1.5418$ Å) on a diffractometer (Rigaku, Japan). The sample for XRD characterization was prepared by placing 20 μL of the suspension on a glass slide. Scanning electron microscopy (SEM) was operated on a field emission microscope (QUANTA 200, FEI Co.). The sample for SEM examination was prepared by placing a drop of the dispersion on a glass substrate and air-dried at room temperature. Transmission electron microscopy (TEM) images were obtained using Tecnai G2 F20 instrument (Philips Holland) equipped with an Energy-dispersive X-ray spectroscopy (EDX) analyzer. A small amount of the sample was dispersed in ethanol, and then a drop of this suspension was deposited on an amorphous carbon film on Cu grid for TEM observation.

3. Results and discussion

3.1. Characterization of the synthesized silver nanowires

The crystalline nature of the bulk nanowires was examined by XRD analysis. Fig. 1 shows the XRD pattern collected. The four diffraction peaks observed ($2\theta = 38.08°$, 44.42°, 64.40° and 77.84°) could be assigned to (1 1 1), (2 0 0), (2 2 0) and (3 1 1) reflection lines of a face-centered cubic crystal of silver [14]. It has been reported that Ag_2S formed at the initial stage would promote the growth process with a “seed catalysis mechanism” [30]. In this study, L-cysteine was chosen as S resource for the formation of Ag_2S to synthesize silver nanowires. The key to the formation of

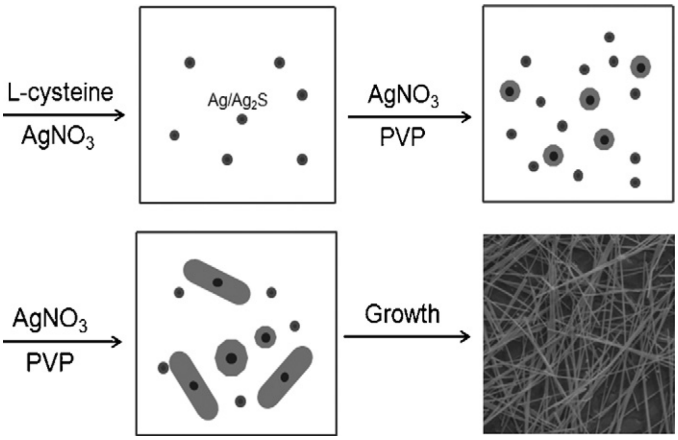

Fig. 2. Schematic illustration of the experimental procedure that generates silver nanowires through an L-cysteine assisted PVP-modified polyol process.

silver nanowires was believed to be the use of PVP as a polymer capping reagent and the introduction of a seeding step. Fig. 2 shows a schematic diagram outlining the plausible mechanism, which can be simply described as follows: When silver nitrate was reduced by EG in the presence of seeds (Ag or Ag_2S particles), silver nanoparticles were generated in the reaction mixture. In terms of surface-energy minimization, when this dispersion of silver nanoparticles was continuously heated at high temperatures, the small nanoparticles progressively disappeared to the benefit of larger ones via a process known as Ostwald ripening [31]. With the assistance of PVP, some of the large nanoparticles were able to grow into rod-shaped structures, which could grow continuously into nanowires, because the side surfaces are tightly passivated by PVP and the ends are largely uncovered and remain to be attractive (or reactive) toward new silver atoms [14]. Actually, further research is needed to illustrate the exact formation of the nanowire structure, which is underway in our group.

The morphologies and sizes of as-prepared products were observed by scanning electron microscopy (SEM) combined with transmission electron microscopy (TEM). Fig. 3A and B demonstrates SEM images of the samples under different magnifications, exhibiting typical nanowire morphologies. Fig. 3C displays a TEM image of the well-defined nanowires, from which it can be seen that the obtained silver nanowires are 300 nm in diameter and up to several tens micrometers in length. And the single-crystal structure was revealed by the selected area electron diffraction (SAED) pattern shown in the inset of Fig. 3C. Furthermore, the energy-dispersive X-ray spectrum (EDS) collected validated the chemical composition of the nanowires. As can be seen in Fig. 3D, the peaks of Ag appear at 3, 22 and 25 together with C and Cu peaks that can be assigned to the carbon film Cu grid used.

3.2. Electrochemical behavior of the Ag NWs/Pt electrode

Fig. 4 demonstrates cyclic voltammograms obtained with Ag NWs/Pt electrode for 5 mM chloride, 5 mM iodide and 5 mM bromide in 0.1 M pH 7.0 PBS. As can be seen, three pairs of well-defined redox peaks were presented, which could be attributed to the formation and the reduction of the three silver compounds (AgCl,

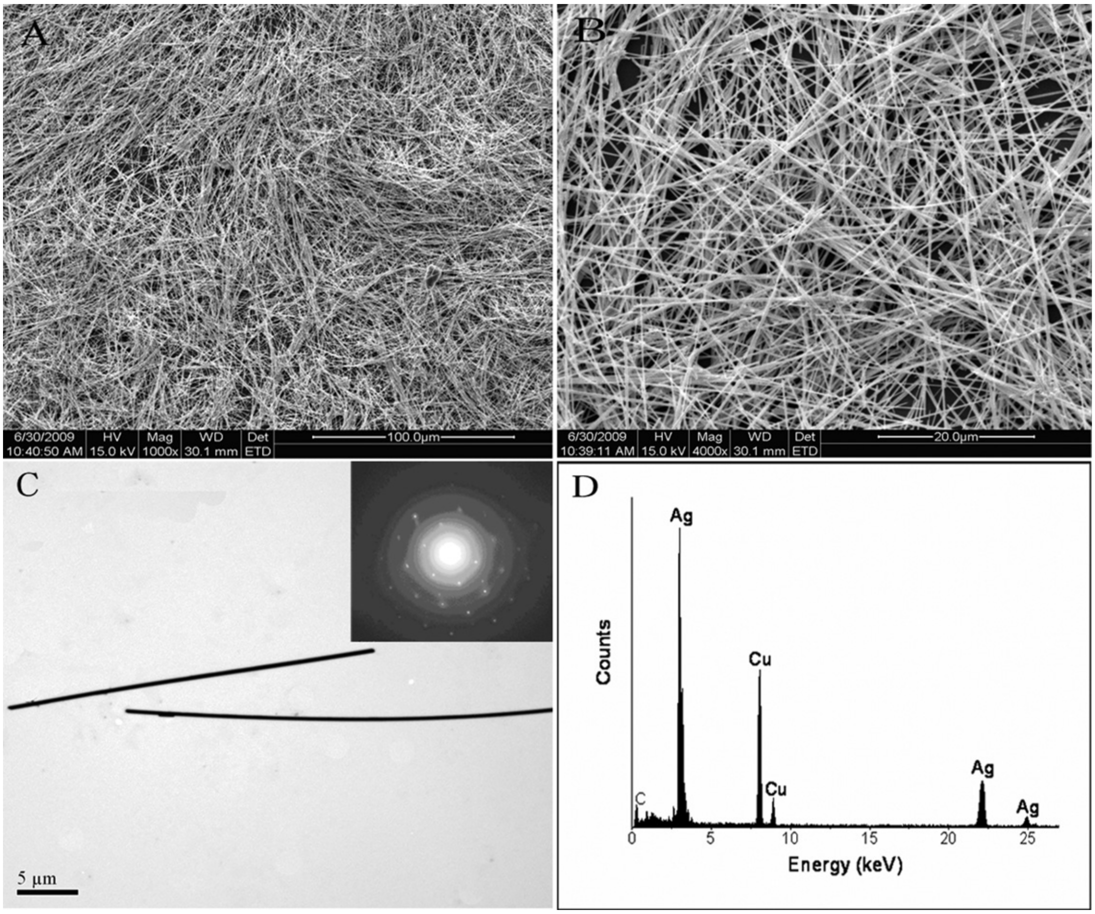

Fig. 3. (A and B) SEM images of the as synthesized silver nanowires under different magnifications, PVP:$AgNO_3$ = 3:1, L-cysteine 1 mM, T = 160 °C, t = 20 min. (C) TEM images and the corresponding SAED (inset). (D) EDS of the nanowires.

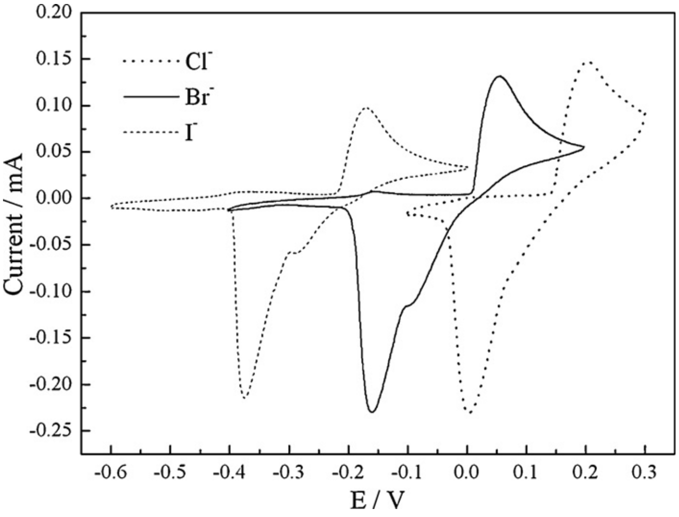

Fig. 4. Cyclic voltammograms of silver nanowires modified Pt electrode in 0.1 M PBS (pH 7.0) with 5 mM chloride, bromide and iodide, respectively, in single solution, scan rate: 50 mV/s.

AgBr and AgI) [28]. It has been well established that when a halide ion such as a chloride, bromide, or iodide ion reacts with the Ag atoms, a silver halide precipitate is formed on the surface and consequently produces an oxidation wave on the voltammogram, while reduction of the silver halide precipitate on the electrode surface leads to generation of a reduction current and correspondingly a reduction wave is produced. The electrochemical reaction can be described by the equation: $AgX + e^- \rightleftharpoons Ag + X^-$ ($X = Cl^-, Br^-, I^-$). And it is found that the difference in the interaction tendency to form silver compounds (the order: AgI > AgBr > AgCl) contributes to the well-separated oxidation/reduction potentials [29], which thus provides a possibility to identify and detect halide ions in a mixture.

From Fig. 4, we can also see that the I_{pc}/I_{pa} value was not equal to unity and the peak potential difference (ΔEp) was more than 200 mV for all the three halides, it is thus expected that it was a pseudo-reversible redox process. Further more, a close view reveals that the reduction current is about twice of oxidation current and there is a minor peak except a central peak during the cathodic sweep. The pre-peak may reflect adsorption of the product at the electrode surface which makes the reduction process more complicated, thus the oxidation process is more precise for the quantification of halide. Fig. 5 shows the plot of $\log(I_{pa})$ vs. $\log(\nu)$. A slope value of ~0.5 was observed for all the three halide ions, that is to say, the oxidation peak current (I_{pa}) was proportional to the square root of the sweep rate ($V^{1/2}$), indicating the oxidation process of the electrode reaction was diffusion-controlled according to the Randles–Sevcik equation [32]: $I_p = 2.69 \times 10^5 AD^{1/2}n^{3/2}V^{1/2}C$, where A, D, n, and C are constant values.

Voltammograms of halide ions with the Ag NWs/Pt electrode were obtained at various pH. At high pH, such as pH 12, the redox waves of silver oxide generated on the Ag surface during the sweep became superimposed on those of AgCl, but not at pH less than 8. Phosphate buffer of pH 7.0 was thus selected as the supporting electrolyte for halide ion determination.

Voltammograms of the halide ions were obtained with different amounts of silver nanowires modified on the electrode in 0.1 M PBS containing 5 mM chloride, iodide and bromide, respectively. The effect of silver nanowire amount on the oxidation peak current is demonstrated in Fig. 6. The oxidation peak current increased as the amount increased, which could be due to the increased silver halide precipitate produced on the electrode surface. Considering that it would easily flow out of the electrode surface while more solu-

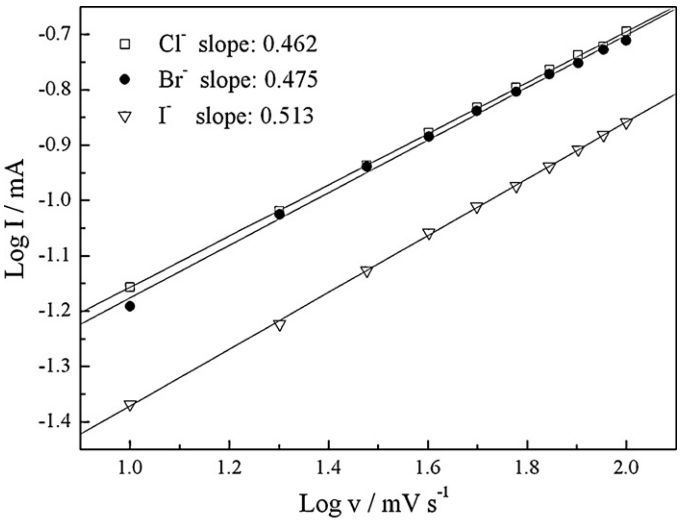

Fig. 5. Plot of $\log(I_{pa})$ vs. $\log(\nu)$ for 5 mM Cl^-, Br^-, and I^-.

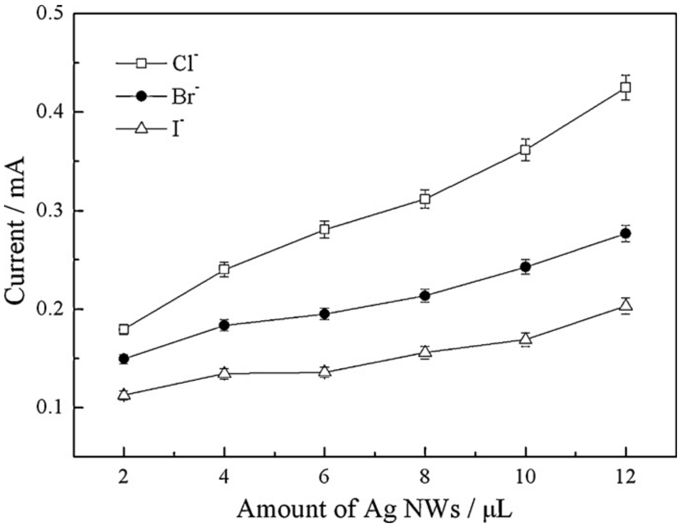

Fig. 6. Effect of amount of silver nanowires used on the responses of the halide ions sensors.

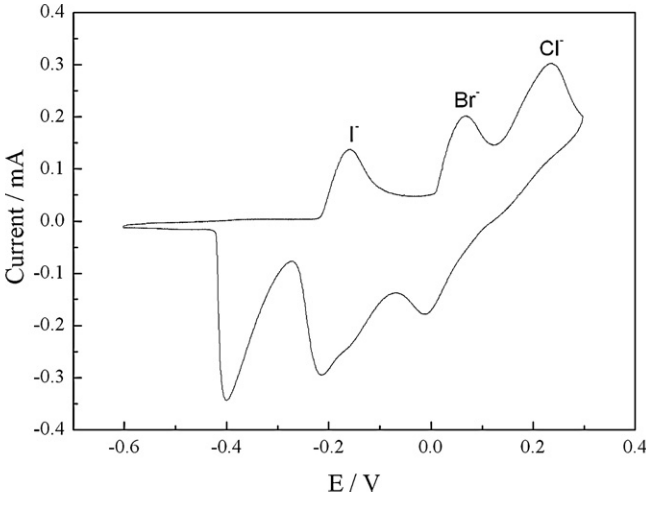

Fig. 7. Cyclic voltammograms obtained with the silver nanowires modified Pt electrode in 0.1 M PBS (pH 7.0) containing 4.2 mM chloride, bromide and iodide, respectively, in a mixed solution at scan rate of 50 mV/s.

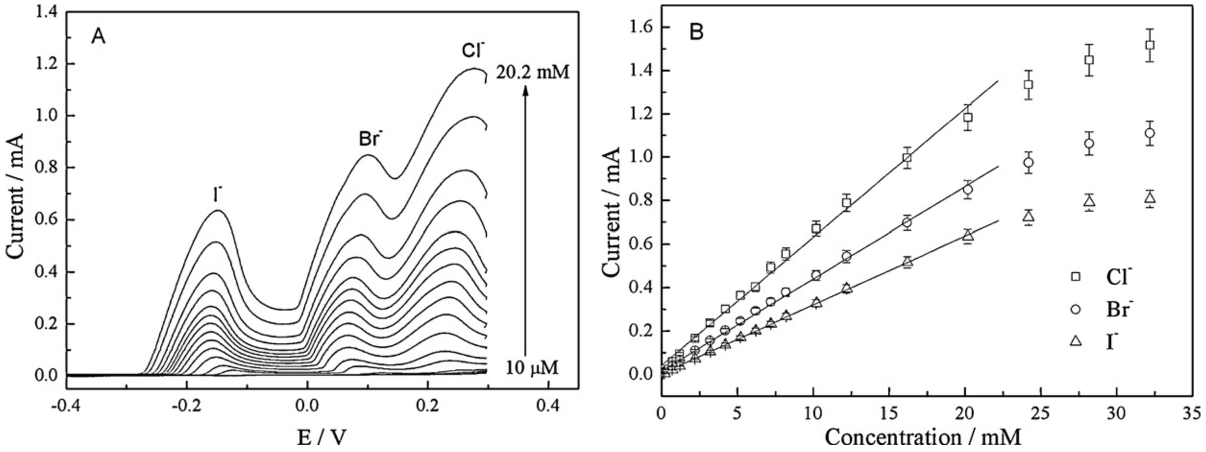

Fig. 8. Simultaneous determination of halide ions at the silver nanowires modified Pt electrode by cyclic voltammetry in 0.1 M PBS (pH 7.0): (A) oxidation waves of the cyclic voltammograms and (B) calibration curves for chloride, bromide, and iodide respectively. Error bars = ±standard deviation ($n = 5$).

tion casted, 8 μL silver nanowire solution was selected for halide sensing in the following experiment.

3.3. Halide ion determination

Since the halide ions possess well-separated redox peak potentials on cyclic voltammograms (Fig. 4), simultaneous determination of Cl^-, Br^- and I^- in aqueous solutions is possible, which is shown in Fig. 7. As can be seen in Fig. 7, the distinguishable electrochemical signals for the halide ions were obtained in a mixed solution of Cl^-, Br^- and I^-, and the peak potentials were in close agreement with those exhibited in Fig. 4, allowing those ions to be identified directly. Fig. 8A shows the oxidation waves of voltammograms upon successive addition of halide from low to high concentrations in a mixture. The calibration curves obtained with the oxidation peak currents are shown in Fig. 8B. The slope of the plot was 0.059, 0.042 and 0.032 (μA/μM) (correlation coefficient = 0.999) for Cl^-, Br^- and I^-, respectively, which were higher than the corresponding values obtained with the screen-printed silver electrode reported by Chiu et al. [29]. In the range of 200 μM to 20.2 mM, 50 μM to 20.2 mM and 50 μM to 20.2 mM for Cl^-, Br^- and I^-, respectively, the current response was proportional to the halide concentrations. The detection limit ($S/N = 3$) was 20 μM, 10 μM and 10 μM for Cl^-, Br^- and I^-, respectively.

The long-term storage stability is evaluated by testing the electrode in halide ion solution (5 mM each) every day. When not in use, the electrode was kept at 4 °C under dry conditions. It retained over 85% of its initial analytical signal for all the three ions after one week of storage, suggesting the stability of the Ag NWs/Pt electrode. The intra- or inter-assay coefficients of variation for five successive determinations of 5 mM chloride and five detections of 5 mM chloride at five electrodes prepared independently were 3.4% and 5.7%, respectively, indicating acceptable reproducibility and repeatability.

The anti-interference ability of the Ag NWs/Pt electrode was also strongly demonstrated against the potential interfering anions. For SO_4^{2-}, NO_3^- and PO_4^{3-}, the interference effect on the oxidation current was insignificant even for 10 times excess of interfering ions to 5 mM Cl^-, 5 mM Br^- and 5 mM I^-. This is as expected due to a relatively bigger solubility of SO_4^{2-}, NO_3^- and PO_4^{3-} than those of the halides in aqueous solutions. As to likely interferents, such as CN^-, SCN^- and S^{2-} that have poorly soluble silver salts, the interference is noticeable even at equal concentration of interfering ions. Especially, the interference effect is −7.34% for CN^- to Cl^-, +19.57% for SCN^- to Br^- and −26.21% for S^{2-} to I^-, when the concentration is 5 mM for all the ions. Fortunately, the amount of CN^-, SCN^- and S^{2-} is often low in real samples and the interference could be negligible when the concentration of interfering ions is 10 times less than the analytes. Thus, the selectivity of Ag NWs/Pt electrode is still acceptable and the proposed sensor can be practically applicable in halide sensing.

Table 1
Recovery of test results of chloride determination in serum by standard addition method.

Sample	Original detected value (mM)	Spike (mM)	Detected value after spike (mM)	Recovery (%) ($n = 5$)
Serum[a]	1.07 ± 0.008	1	2.09 ± 0.015	102.80 ± 0.84
		2	3.16 ± 0.019	104.71 ± 0.75
		3	4.23 ± 0.016	105.47 ± 0.56
		4	5.28 ± 0.013	105.35 ± 0.45

[a] Dilution factor = 100.

Real sample analysis of Cl^- in serum and that spiked with standard solutions was presented in this study. Mean values and the recoveries obtained by standard addition method are shown in Table 1. Serum was taken from a healthy person and the concentration of chloride value measured was 106.8 ± 0.83 mM, which was in close agreement with the value of 106 mM provided with the ISE method at a local hospital. From the results in Table 1, it is obvious that good recovery values (accuracy) are given, indicating that the proposed method can be applicable in real sample determination.

4. Conclusions

In conclusion, a voltammetric method for sensitive and selective determination of halide ions was described, using the silver nanowires modified Pt electrode as a sensing probe. Silver nanowires were synthesized by an L-cysteine-assisted PVP-mediated polyol route. Data collected from the voltammetric experiments show that the performance of the fabricated sensor makes it suitable for quantitative detection of chloride, bromide and iodide in terms of sensitivity, selectivity, linear range and detection limit. Some of the general advantages of this work include: (1) the high effective surface area and fast electron transfer rate from the nanowire structure, (2) distinguishable electrochemical signals from the well-separated redox peaks to identify halide ions easily and (3) a simple approach that affords microsensor format. This proposed Ag NWs/Pt electrode is not only promising for halide analyses but also offer potential applicability for hydrogen peroxide sensing, glucose detection, and so forth.

Acknowledgments

The financial supports from National Natural Science Foundation of China (Grant Nos. 30900325, 30772746 and 30870665) and Natural Science Foundation of Tianjin (Grant No. 08JCZDJC20600) are well acknowledged.

References

[1] Y. Bi, G. Lu, Chem. Mater. 20 (2008) 1224–1226.
[2] A.P. Lynn, E.V. Amy, P.B. Andrew, M.D. Robert, Science 291 (2001) 103.
[3] X. Wen, Y. Xie, W.C. Mak, K.Y. Cheung, X. Li, R. Renneberg, S. Yang, Langmuir 22 (2006) 4836–4842.
[4] J. Riu, A. Maroto, F.X. Rius, Talanta 69 (2006) 288–301.
[5] M.L. Charles, L.W. Zhong, MRS Bull. 32 (2007) 99–108.
[6] C. Jagadish, Semicond. Sci. Technol. 25 (2010) 1.
[7] V.P. Menon, C.R. Martin, Anal. Chem. 67 (1995) 1920–1928.
[8] M.H. Yang, F.L. Qu, Y.S. Lu, Y. He, G.L. Shen, R.Q. Yu, Biomaterials 27 (2006) 5944–5950.
[9] H.C. Wang, X.S. Wang, X.Q. Zhang, X. Qin, Z.Z. Zhao, Z.Y. Miao, N. Huang, Q. Chen, Biosens. Bioelectron. 25 (2009) 142–146.
[10] S.M. Choi, J.H. Kim, J.Y. Jung, E.Y. Yoon, W.B. Kim, Electrochim. Acta 53 (2008) 5804–5811.
[11] F.L. Qu, M.H. Yang, G.L. Shen, R.Q. Yu, Biosens. Bioelectron. 22 (2007) 1749–1755.
[12] A. Govindaraj, B.C. Satishkumar, C.N.R.R.M. Nath, Chem. Mater. 12 (2000) 202–205.
[13] Y.J. Han, J.M. Kim, G.D. Stucky, Chem. Mater. 12 (2000) 2068–2069.
[14] Y.G. Sun, B. Mayers, T. Herricks, Y.N. Xia, Nano Lett. 3 (2003) 955–960.
[15] P. Jiang, S.L. Li, S.S. Xie, Y. Gao, L. Song, J. Chem. Eur. 10 (2004) 4817–4821.
[16] T. Katsu, Y. Mori, N. Matsuka, Y. Gomita, J. Pharm. Biomed. Anal. 15 (1997) 1829–1832.
[17] C. Huber, T. Werner, C. Krause, I. Klimant, O.S. Wolfbeis, Anal. Chim. Acta 364 (1998) 143–151.
[18] T. Masadome, Y. Asano, T. Nakamura, Talanta 50 (1999) 595–600.
[19] E. Colt, H.H. Nishi, Clin. Chem. 7 (1961) 285–291.
[20] O. Shales, S.S. Shales, J. Biol. Chem. 140 (1941) 879–884.
[21] E. Bakker, Y. Qin, Anal. Chem. 78 (2006) 3965–3983.
[22] F. Faridbod, M.R. Ganjali, R. Dinarvand, P. Norouzi, Sensors 8 (2008) 2331–2412.
[23] R. Zielinska, E. Mulik, A. Michalska, S. Achmatowicz, M. Maj-Zurawska, Anal. Chim. Acta 451 (2002) 243–249.
[24] J.F. Huang, Talanta 77 (2009) 1694–1700.
[25] R. Michalitsch, P.E. Laibinis, Angew. Chem. Int. Ed. 40 (2001) 941–944.
[26] R. Michalitsch, B.J. Palmer, P.E. Laibinis, Langmuir 16 (2000) 6533–6540.
[27] H.G. Choi, P.E. Laibinis, Anal. Chem. 76 (2004) 5911–5917.
[28] K. Arai, F. Kusu, N. Noguchi, K. Takamura, H. Osawa, Anal. Biochem. 240 (1996) 109–113.
[29] M.H. Chiu, W.L. Cheng, G. Muthuraman, C.T. Hsu, H.H. Chung, J.M. Zen, Biosens. Bioelectron. 24 (2009) 3008–3013.
[30] C. Chen, L. Wang, H.J. Yu, J.J. Wang, J.F. Zhou, Q.H. Tan, L.B. Deng, Nanotechnology 18 (2007) 115612–115618.
[31] E. Matijevic, Chem. Mater. 5 (1993) 412–426.
[32] S. Hrapovic, Y.L. Liu, K.B. Male, J.H.T. Luong, Anal. Chem. 76 (2004) 1083–1088.